

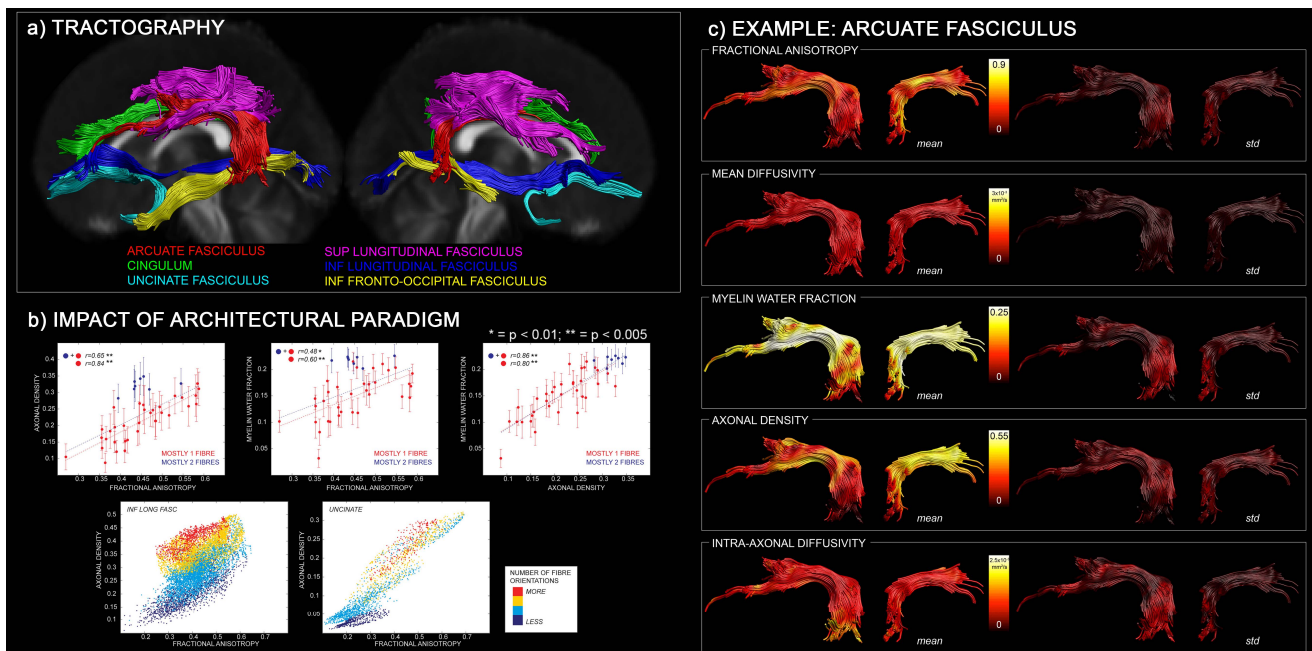
# The CONNECT brain atlas of white matter microstructure

Silvia De Santis<sup>1</sup>, Yaniv Assaf<sup>2</sup>, Sonya Bells<sup>1</sup>, Sean C Deoni<sup>3</sup>, and Derek K Jones<sup>1</sup>

<sup>1</sup>CUBRIC Cardiff University, Cardiff, United Kingdom, <sup>2</sup>Department of Neurobiology, Tel Aviv University, Tel Aviv, Israel, <sup>3</sup>School of Engineering, Advanced Baby Imaging Lab Brown University, Providence, RI, United States

**INTRODUCTION AND TARGET:** While diffusion tensor MRI (DT-MRI) has proven to be an incredibly useful tool over recent years, DT-MRI indices have a notorious lack of specificity to specific sub-components of white matter (WM) microstructure. Axonal membranes play the primary role in determining fractional anisotropy (FA), but myelination also modulates FA [1]. Moreover, the fibre *architectural paradigm* has a huge impact where intra-voxel orientational dispersion of fibre populations leads to a reduction in the measured FA. Lastly, water diffusivity parallel to the axon will also modulate FA. Understanding the role of WM microstructure in brain function in health and disease demands more specific indices that tap into these sub-components. Moreover, it is imperative that we first understand how these different parameters vary across different brain regions and fibre pathways, and how they differ between individuals. To this end, over the last 2 years, we have been developing **the first microstructural atlas** that includes both DT-MRI and advanced microstructural indices. The CHARMED model [2] provides estimates of the axonal density (AD) and the intra-axonal longitudinal diffusivity (IAD); the mcDESPOT analysis provides the myelin water fraction (MWF) [3] and HARDI methods allow the fibre orientation density function to be estimated [4]. The atlas includes population means and standard deviations of multi-variate data for every voxel in MNI space, and for all major association, projection and commissural pathways which can be described and differentiated on the basis of their microstructural properties, and is meant to serve as a reference for all the experimenters interested in microstructural imaging.

**METHODS:** 17 healthy volunteers, (mean age/std.dev.=24/3y), underwent an MRI protocol at 3T comprising: cardiac-gated DT-MRI (TE=93ms, 45 dirs, max b-value=1200s/mm<sup>2</sup>), CHARMED protocol (TE/TR=114/17000ms, 130 dirs, max b-value=7500s/mm<sup>2</sup>) [5], mcDESPOT (SPGRs: TE/TR=2.1/4.7ms, flip angle(a)=[3,4,5,6,7,9,13,18]; bSSFPs: TE/TR=1.6/3.2ms, a=[10.6,14.1,18.5,23.8,29.1,35.3,45,60]) and high resolution T<sub>1</sub>-weighted anatomical scan (FSPGR). DT-MRI analysis was performed with *ExploreDTI* to obtain FA/MD maps [6]. Whole brain tractography was obtained for each subject in native space using constrained spherical harmonic deconvolution [4]. Waypoints were then defined to virtually dissect the cingulum, arcuate, uncinate, superior longitudinal, inferior longitudinal and inferior fronto-occipital fasciculi in each hemisphere. A 'binarized' map was computed for each reconstructed fasciculus, with the same matrix size as the FA, but one if the voxel is intersected by a streamline, zero elsewhere. CHARMED [2] and McDESPOT [3] analyses were coded in Matlab/C++ to obtain maps of AD, IAD and MWF. For each subject, all the parametric maps were non-linearly registered to the T<sub>1</sub>-weighted anatomical scan. The latter was used to normalize the brain in MNI space again via non-linear warping. The combined transformations were then applied to the parametric maps and to the binarised tract maps. Population mean and standard deviation were calculated in each voxel for all parameters. The 'probabilistic' overlay of binarized tract maps was computed for each tract and thresholded at 70% (i.e., ≥ 70% of population had a streamline passing through the voxel), which we refer to as a 'tract commonality map'. The entire set of streamlines from a whole brain tractography result of one subject was then warped non-linearly to MNI space. Only the portions of streamlines passing through non-zero voxels in the tract commonality map for each tract were retained for the fibre atlas. Finally, the multi-parametric voxel-wise data were analysed by harvesting data from the intersection of the FA-derived skeleton from the tract-based spatial statistics pipeline and standardized WM labels in standard space.



**RESULTS AND DISCUSSION:** Fig. 1a. shows the representative pathways obtained after filtering with the tract commonality map. Fig. 1b shows the impact of different architectural paradigms (# fibre orientations) on parameters derived from DT-MRI and on more advanced techniques like CHARMED. While FA is clearly dependent on the number of main fibre orientations in the voxel, so that fibre dispersion lowers the FA, AD shows independence, and hence provides a more direct measure of axonal properties. Accounting for # fibre populations allows better interpretation of the correlation between FA and MWF, which is much stronger if only single fibre population regions are selected. Since AD is independent of # fibre populations, it has the highest correlation with MWF. Fig. 1c shows an example normalized tract, the arcuate fasciculus. For each tract, mean values, standard deviations and correlations between the parametric maps (FA, MD, AD, IAD, MWF) are provided. Moreover, the distribution of the population mean and the standard deviation of the parameters are displayed along the tract.

**CONCLUSION:** We have produced the first microstructural atlas of WM in standard space, including measures of myelination, axonal density and axonal diffusivity along tracts. Combining advanced techniques allow a better understanding of the contrast underpinning conventional DT-MRI and holds great promise for increasing the specificity of diffusion MRI in health and disease. **ACKNOWLEDGEMENTS:** EU-FP7 FET which supported the CONNECT consortium.

**REFERENCES:** [1] Beaulieu C *NMR Biomed.* **15**:435 (2002) [2] Assaf and Basser *MRM* **52**:965 (2004); [3] Deoni et al. *MRM* **60**:1372 (2008); [4] Tournier JD et al. *Neuroimage* **23**:1176 (2004) [5] De Santis et al. *Proc. ISMRM* (2011) [6] Leemans et al. *Proc. ISMRM* (2009)